

# A New OEO Design Using Optical Phase Modulation and Modulation Suppression

G. John Dick and Nan Yu  
Jet Propulsion Laboratory, California Institute of Technology  
Pasadena, CA 91109-8099, U.S.A  
Email: john.dick@jpl.nasa.gov

**Abstract**— We present the design for a phase-modulated Opto-Electronic Oscillator (OEO) that incorporates asymmetric Mach-Zehnder (AMZ) interferometers as phase demodulators together with PM modulation suppression. The new design promises to obtain in the electro-optical domain the low-noise advantages previously achieved in RF and microwave oscillators by the use of carrier suppression but which have been achieved only to a limited extent in OEO's.

## I. INTRODUCTION

OEO designs using RF carrier suppression have already been demonstrated [1], and they do show the rejection of amplifier flicker noise as is shown in microwave oscillator and interferometer applications [2]. However, a second important advantage of microwave carrier suppression, the reduction of the effects of thermal- or shot-noise [3], has not been realized in an OEO application before now. This second reduction is made possible in microwave applications by the use of higher power levels in the oscillator or interferometer than can be tolerated by a low-noise follower amplifier, combined with a means for reducing the power at the detector that still preserves the systems sensitivity i.e. without reducing the output response to phase variation induced by the resonator discriminator or component under test.

The design presented here realizes this second advantage for the first time in the opto-electronic arena by enabling the effective use of high optical power levels to reduce shot-noise induced frequency variation in an OEO. This is done by use of an Asymmetric Mach-Zehnder (AMZ) phase demodulator (phase detector) with unbalanced outputs together with modulation suppression. With appropriate delays and phases, the AMZ demodulator can transmit virtually all of the optical power to a terminated output port while a signal with suppressed optical carrier but with high sensitivity to input PM is developed at the other port. Sideband amplitude also is reduced before detection by use of a phase un-modulator (matched to a PM modulator that replaces the AM unit used in a typical OEO). This reduction of both carrier and sidebands combines to prevent overload of the low-noise optical detector (which always has a low optical saturation power) as optical power is increased.

## II. OEO DESIGN WITH PM MODULATION SUPPRESSION

Figure 1 shows an overall block diagram for the OEO design. It consists of two parts which are separated by dashed containing boxes. The left box contains a completely self-contained phase-modulated OEO with an available electrical tuning signal input. It consists of a low-noise CW laser, microwave phase modulator, delay line, phase detector (AMZ Phase Demodulator), mode selection filter, electrically variable phase shifter, and a power amplifier to drive the modulator.

The OEO in the left (dashed) box in Figure 1 operates in a manner identical to that of conventional OEOs: Identical, that is, except for the use of phase modulation (a PMOEO) instead of amplitude modulation, and except for the use of a high-powered laser, so that only a fraction of the power need be tapped for use by the oscillator itself. The right half of Figure 1 shows the added modulation-suppressed noise reduction system that senses and corrects for frequency noise in the PM OEO on the left. The use of added noise reduction stages to OEO oscillators is also similar to previous designs [1] which have used stages with carrier-suppressed RF electronics to reduce the noise contributions of RF components in an active OEO oscillator. These added stages work by sensing the frequency error with lower noise than is practical in an active oscillator, and then undo the effects of that noise with feedback. The present unit also works in this way.

However, instead of improving only the performance of RF components, the present noise reduction system also reduces noise inherent in the optical detector itself. The scheme improves performance in two ways; first by enabling the use of very high optical power levels to reduce thermal- and photon shot-noise contributions to the system frequency fluctuations; and secondly by allowing larger modulation levels than would otherwise be possible. Part of the solution is in the AMZ phase demodulators, which will be discussed in the next section and which can be arranged to provide a reduced signal to a low-noise optical detector (thus preventing overloading) while still preserving a high sensitivity to phase modulations on the optical signal. However, what must be measured is the variation of the phase of the phase modulation that is applied to the optical signal, and not the modulation itself, which would overload the detector. So, to enable a high sensitivity with the



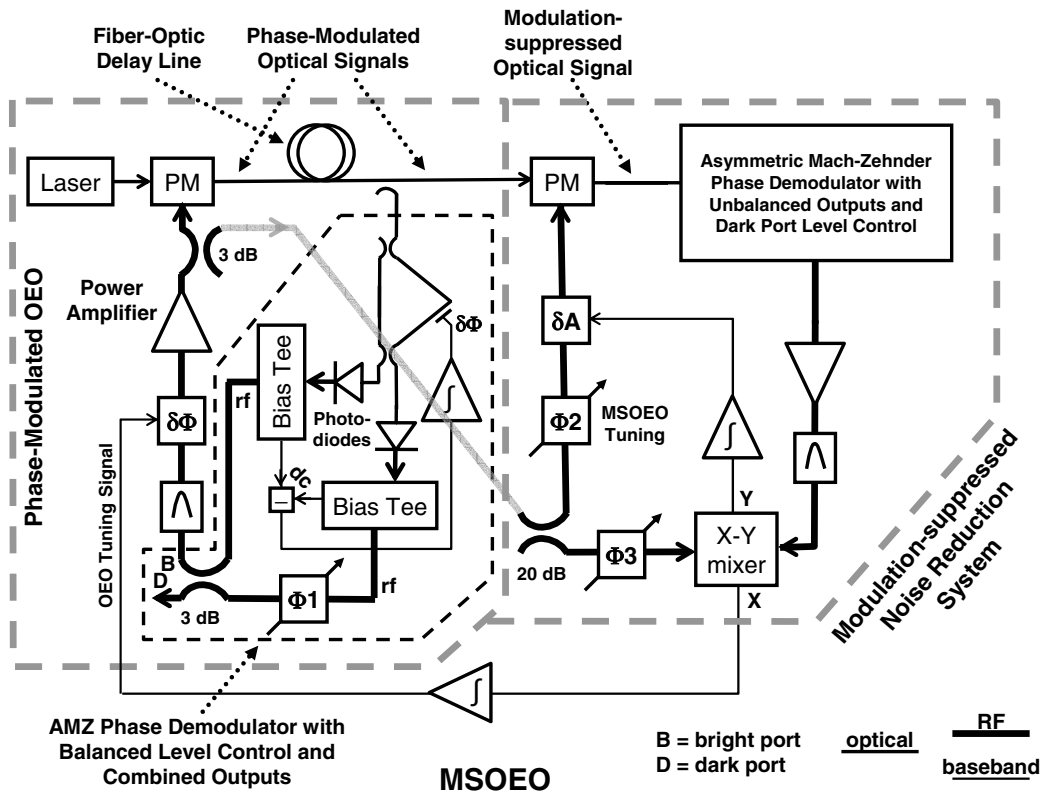


Fig. 2. Diagram of the MSOEO with an expanded view of the AMZ phase demodulator in the tuneable PM OEO subsystem.

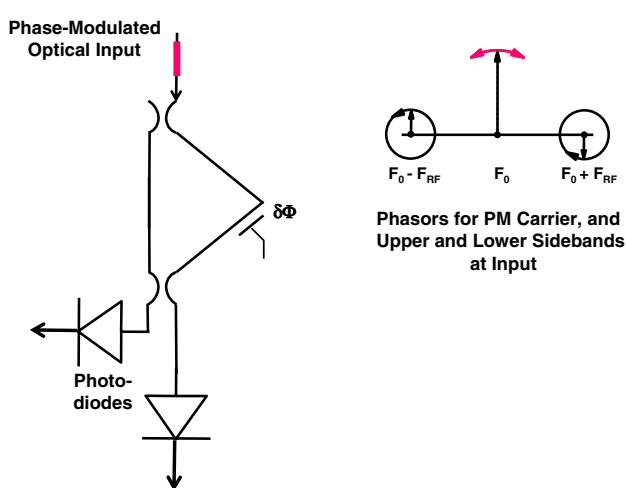


Fig. 3. Phase modulation at the input to the Mach-Zehnder interferometer can be represented by Phasors for the carrier, and for upper and lower sidebands. Higher sidebands also contribute, giving the curved oscillatory path for the phasor as shown by the double arrow.

sense of the phase modulation of the right (red) signals with respect to those on the left (green). When combined with a  $\pi/2$  phase difference between the optical phases (represented here by the 90 degree angular rotation between red and green signal phasors in Fig. 5) the phase modulation at the input is converted into amplitude modulation at the output of the lower

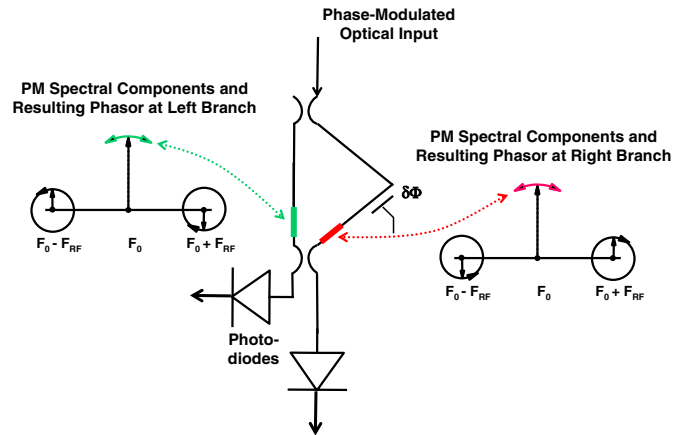


Fig. 4. Added length of the right arm of the interferometer gives a 180 degree phase shift between the phase modulations in the two arms before they are re-combined at the output.

hybrid (blue and orange phasors).

If the optical phase, as adjusted by the optical phase shifter,  $\delta\Phi$  in Figure 6, is not correctly adjusted the RF amplitudes at the two outputs are unbalanced and the DC levels are also unequal. This is indicated by the graph in the inset which shows the (RF) time evolution of the voltage two outputs together with DC levels (dashed lines). As shown in Figure 7, the difference between these voltages is applied to an

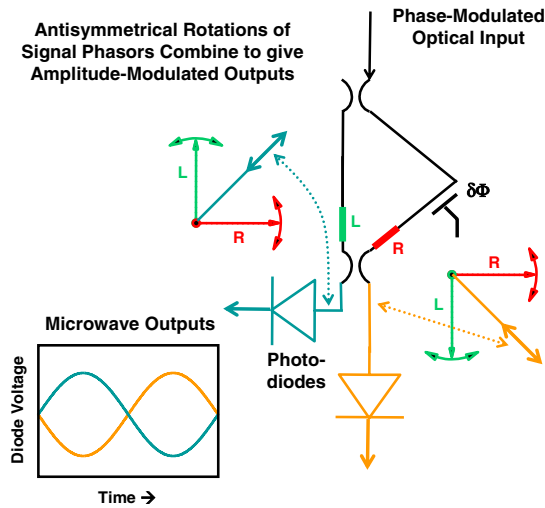


Fig. 5. “Out-of-phase” optical phase modulations in the left and right branches of the interferometer combine to give amplitude modulated signals at its outputs. Detector outputs also show a 180 degree phase difference, as shown in the graph inset.

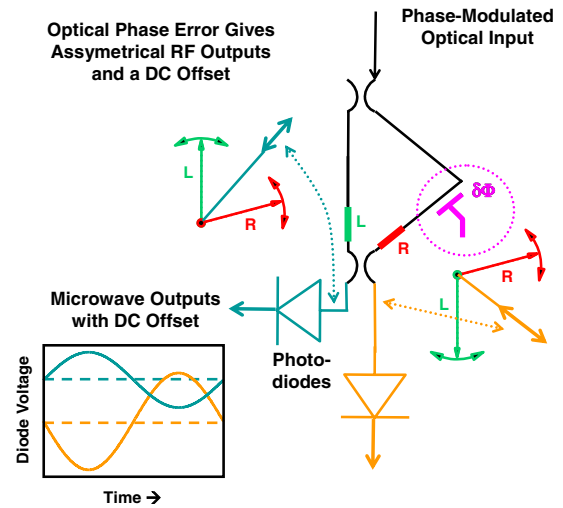


Fig. 6. Improper adjustment of the optical phase delay in the right arm rotates its output phasor, giving rise to unbalanced RF outputs and a DC offset between them as shown in the graph inset.

integrating amplifier in a control loop to continuously adjust the optical phase and so to preserve the  $\pi/2$  optical phase difference between the two arms.

#### IV. AMZ DEMODULATOR WITH UNBALANCED OUTPUTS

Figure 8 shows the overall schematic diagram for the PMOEO with details filled in for the AMZ demodulator in the noise reduction subsystem. Where the AMZ demodulator previously described in the PMOEO receives only a small fraction of the optical power in order not to overload its optical detectors, the full optical power is applied (after passing through the PM un-modulator) to the demodulator on the right.

This second AMZ demodulator operates in a manner similar to the one used in the PMOEO, except that the optical phase is adjusted so that one of the outputs is much smaller than the other. For this case, virtually all of the signal power from a small input phase modulation appears at the low-power (dark) port while all of the optical power appears at the other (bright) port. The bright port is terminated to absorb the optical power without unwanted reflections, while the signal at the dark port is optically detected and then (as in the balanced AMZ demodulator described above) split into a baseband signal that is used to control the optical phase in the interferometer, and an RF signal that is sent on to the quadrature RF detector.

This configuration (modulation suppression plus unbalanced AMZ demodulator) allows the use of high optical power levels without overloading the optical detector in the demodulator and also gives increased sensitivity to phase variations in the optical PM signal from the delay line due to the use of higher optical power and the high sensitivity at the dark port of the unbalanced AMZ demodulator

As shown in Figure 9, this AMZ demodulator is adjusted with optical phase to give unbalanced outputs, a bright port

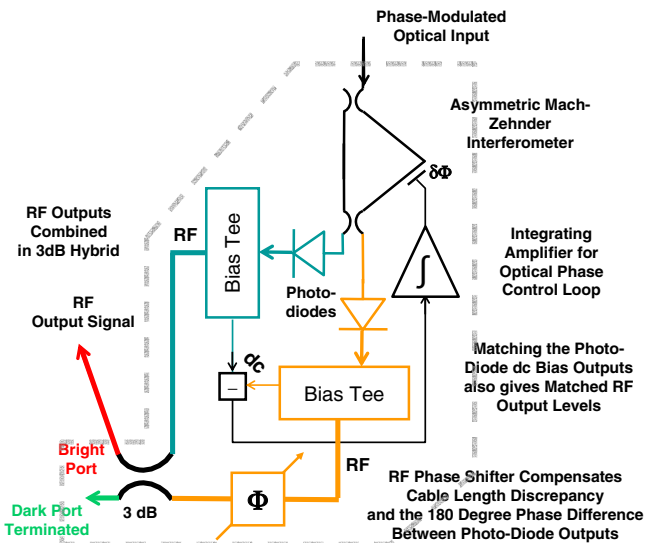


Fig. 7. Detailed block diagram for the Asymmetric Mach-Zehnder Demodulator with Balanced Outputs.

labeled B and a dark port D which presents an optical signal with amplitude that is very sensitive to any input phase modulation. Because this modulation is always nominally zero due to the feedback discussed in the first section, only a very small optical carrier is required at the dark port. The DC bias at the output of the photo-diode detector reflects this carrier level, and is compared with a baseband signal level and integrated to keep the optical phase at a proper value.

Fig. 9 also shows how the optical phase  $\delta\Phi$  can be adjusted to provide a small signal with large amplitude modulation at a dark port. Time dependence of the signal amplitudes is shown in the inset graphs which show the variation at the RF modulation frequency together with DC level values.

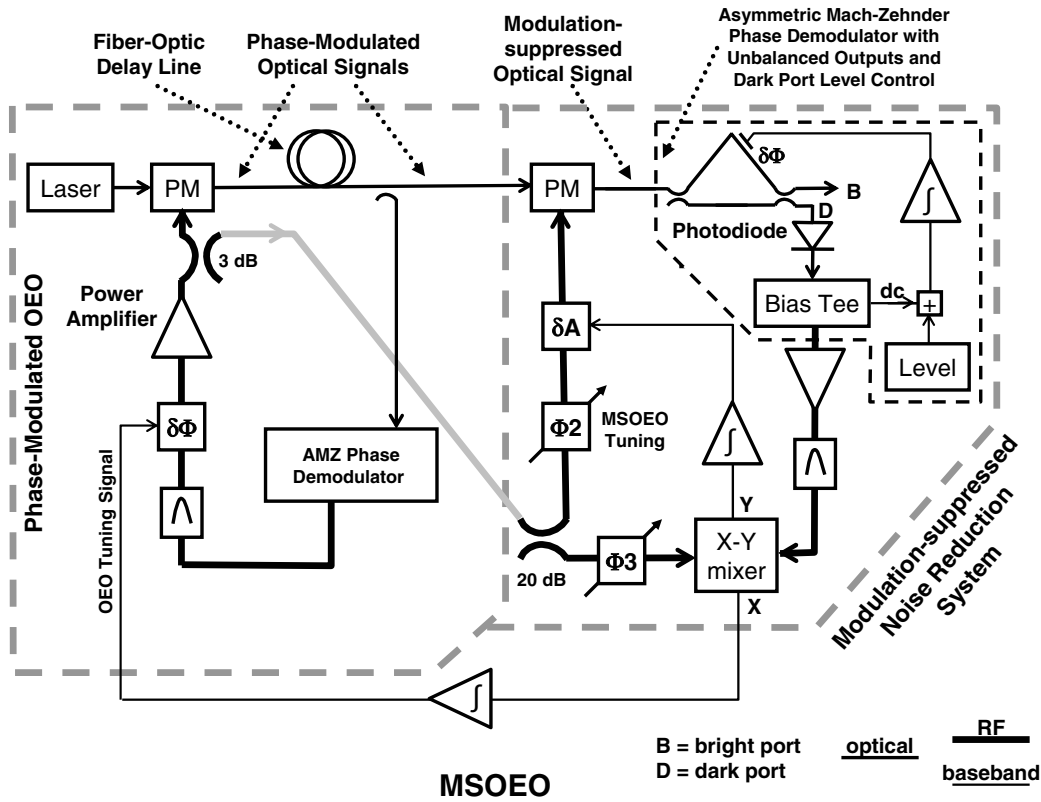


Fig. 8. Modulation-Suppressed OEO with an expanded view of the AMZ Demodulator in the Noise Reduction Subsystem.

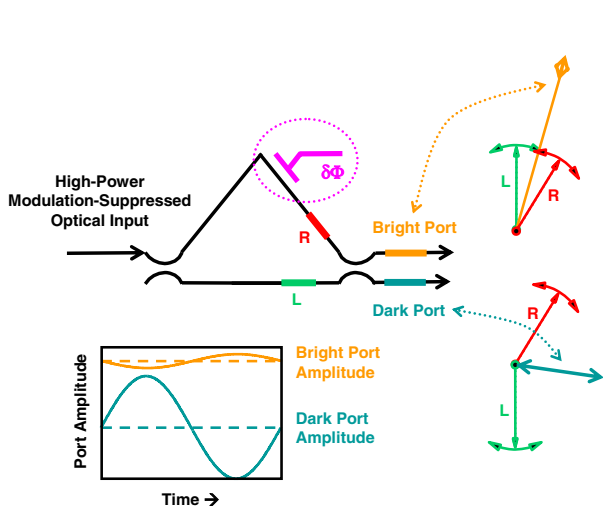


Fig. 9. In order to advantageously accommodate a large optical input  $P$  the optical phase is adjusted so that most of the power goes to one (B) port while most of the signal strength goes to the other (Dark) port.

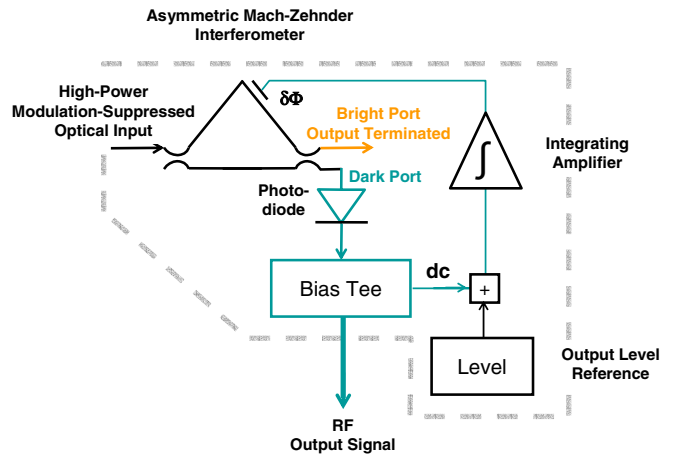


Fig. 10. Detailed block diagram of the AMZ demodulator with unbalanced outputs and dark port level control.

As in the previous phasor diagrams, the angular oscillations (at the RF frequency) of the red and green phasors in Figure 9 are 180 degrees out of phase due to the  $\lambda_{rf}/2$  difference in the lengths of the arms in the interferometer. That is, as the red phasor rotates to the left, the green one rotates to the right, and vice versa. As indicated in the diagrams,

the output port phasors are the vector sums of the input phasors with appropriate (quadrature) phase shifts. By proper adjustment of the optical phase  $\delta\Phi$  the bright port sum phasor (yellow) is shown to have a large length but a small variation due to oscillation of the input phases, while the dark port output phasor (blue) shows a smaller value but a much larger oscillation. These are represented in the time variation shown in the inset graph, where the average values are also shown as dashed lines.

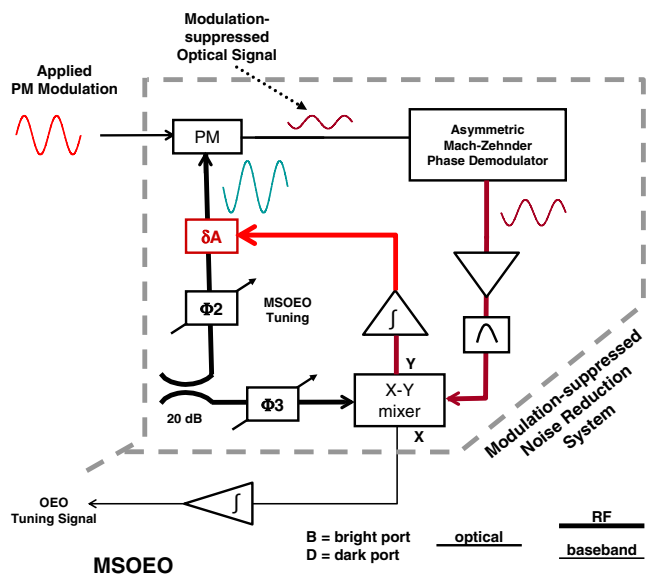


Fig. 11. Expanded diagram for the Modulation Suppressed Noise Reduction System, showing how an error in the amplitude of the unmodulating signal is corrected by a feedback loop incorporating the “Y” port of the X–Y mixer

The magnitudes of the phase oscillations are shown much enhanced in Figure 9. Due to the effect of modulation suppression, only a remnant noise phase modulation (at the RF frequency) would remain at the input to the unbalanced AMZ demodulator. This allows the use of a very small remnant carrier in the dark port and thus an input power that is very much larger than that which the photo-diode detector, as shown in Figure 10, can withstand.

Figures 11 and 12 show how errors in the amplitude and phase of the un-modulating signal are detected and corrected. For the case of amplitude error as shown in Fig. 11, the resulting (small) phase modulation is approximately in phase with the applied modulation signal and is detected and corrected with an integrator through the “Y” port of the X–Y mixer. On the other hand, if phase shifter  $\Phi 2$  is adjusted as illustrated in Fig. 12 (or if the PM OEO fluctuates from the proper frequency) the consequent phase error is corrected by tuning the frequency of the PM OEO, thus reducing its frequency fluctuations while also providing a means for tuning the frequency of the combined oscillator.

## V. CONCLUSIONS

Designs have been developed and presented for a new phase-modulated optoelectronic oscillator with a modulation-suppressed noise reduction subsystem, and for optical phase demodulators that enable advantageous application of high optical powers without overloading the optical detectors. The use of modulation suppression allows a reduction for the first time in an OEO for shot noise at the detectors; taking advantage of higher available optical power and larger phase modulation amplitude.

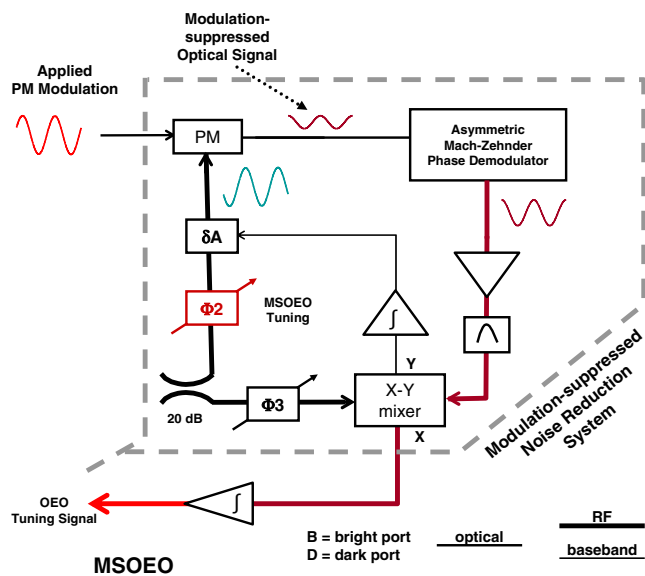


Fig. 12. Expanded diagram as in Fig. 11 but with an error in the phase of the unmodulating signal resulting in correction of the frequency of the PM OEO by means of a loop involving the “X” port of the X–Y mixer. In this case the phase of the (small) PM modulation-suppressed error signal is shifted by approximately 90 degrees from that of the applied signals.

The new demodulator design works by use of an asymmetric Mach–Zehnder interferometer with an approximate  $\lambda_{rf}/2$  length difference to invert the modulations in the arms before re-combining; operating in with asymmetric outputs allows the high optical power to be effectively separated from a small optical error signal used to null the modulation cancellation and to correct frequency fluctuations in the PM OEO.

## ACKNOWLEDGMENTS

This work was carried out at the Jet Propulsion Laboratory, California Institute of Technology under a contract with the National Aeronautics and Space Administration.

## REFERENCES

- [1] X. Steve Yao, Lute Maleki, and G. John Dick, “Opto-Electronic Oscillator Incorporating Carrier Suppression Noise Reduction Technique,” *Proceedings, 1999 Joint Meeting of The European Frequency and Time Forum and IEEE International Frequency Control Symposium*, 565–566, 1999, also see *JPL New Technology Report NPO-20546*.
- [2] For example, see E. N. Ivanov, M. E. Tobar, and R. A. Woode, “Advanced Phase Noise Suppression technique for the next generation of Ultra-Low Noise Microwave Oscillators,” *Proceedings, 49th IEEE Freq Control Symposium*, 314–320 1995.
- [3] A. Sen Gupta, D. A. Howe, C. Nelson, A. Hati, F. L. Walls, and J. F. Nava, “High-Spectral-Purity Microwave Oscillator: Design Using Conventional Air-Dielectric Cavity,” *Proceedings, 2003 IEEE International Frequency Control Symposium and PDA Exhibition jointly with the 17th European Frequency and Time Forum*, 423–430, 2003.